

Freeze-thaw durability of glass textile-reinforced mortar composites

A. Dalalbashi

Department of Civil Engineering, ISISE, University of Minho, Guimarães, Portugal

B. Ghiassi

Centre for Structural Engineering and Informatics, Faculty of Engineering, University of Nottingham, Nottingham, UK

D.V. Oliveira

Department of Civil Engineering, ISISE & IB-S, University of Minho, Guimarães, Portugal

ABSTRACT: Application of textile-reinforced mortars (TRMs) for externally bonded reinforcement of existing masonry structures has received a considerable recent attention. The mechanical behaviour of these composites, which are composed of continuous fibers embedded in an organic matrix, and their effectiveness in improving the performance of strengthened structures are highly dependent on the fiber-to-mortar bond behaviour as well as the bond between TRM system and substrate.

Understanding the long-term performance of these mechanisms is therefore of critical importance for design of durable TRM composites and ensuring the safety of strengthened structures. To address this aspect, the effect of freeze-thaw cycles on the textile-to-mortar bond behaviour is experimentally investigated and discussed in this paper. The results illustrate a significant deterioration of the textile-to-mortar bond performance in the studied composites.

1 INTRODUCTION

The advantages of textile reinforced mortar (TRM) composites with respect to fiber-reinforced polymers (FRPs) have made the former very interesting for externally bonded reinforcement of masonry and reinforced concrete structures (Carozzi & Poggi, 2015; Papanicolaou, Triantafyllou, Papathanasiou, & Karlos, 2007; Razavizadeh, Ghiassi, & Oliveira, 2014).

Composed of continuous fibers embedded in a matrix, TRMs show a pseudo-ductile response with distributed cracking when designed appropriately, which makes them interesting for seismic strengthening applications. The large variety of available fibers and mortar types allow development of TRM composites with a large range of mechanical properties (D'Antino & Papanicolaou, 2017; Donnini, Chiappini, Lancioni, & Corinaldesi, 2019; Mazzuca, Hadad, Ombres, & Nanni, 2019; Younis & Ebead, 2018).

The important role of fabric-to-mortar bond behavior on the post cracking response and strength of these composites has been previously discussed in several recent studies by the authors (Dalalbashi, Ghiassi, Oliveira, & Freitas, 2018a, 2018b; Dalalbashi, Ghiassi, & Oliveira, 2019; Ghiassi, Oliveira, Marques, Soares, & Maljaee, 2016).

While several recent studies have addressed the short-term mechanical performance of TRM composites at different levels, their long-term performance and durability under environmental conditions (Ghiassi

et al., 2015; Maljaee, Ghiassi, Lourenço, & Oliveira, 2016) is very poorly addressed (Al-jaberi & Myers, 2018; Heshmati, Haghani, & Al-Emrani, 2017; Maljaee et al., 2016). This study is aimed at addressing this gap and presents an experimental investigation on the degradation of the fabric-to-mortar bond behavior in TRM composites under freeze-thaw cycles. The tests include exposing the samples to 360 freeze-thaw cycles and evaluating the changes of the mechanical properties of the material constituents and the bond behavior through performing appropriate mechanical characterization tests.

2 EXPERIMENTAL PROGRAM

The experimental program consisted of a series of glass-based TRM composites exposed to the freeze-thaw conditions. The specimens were taken from the climatic chamber after different periods of exposure in order to examine possible changes in the textile-to-mortar bond behavior as well as in the mechanical properties of the fiber and the mortar. In addition, control specimens cured in environmental lab conditions were used to compare results with specimens exposed to freeze-thaw actions.

2.1 Materials characterization tests

A commercially available hydraulic lime-based mortar (Planitop HDM Restauro) was used as

matrix. A high-ductility hydraulic lime mortar is prepared by mixing the powder with the liquid provided by the manufacturer in a low-speed mechanical mixer to form a homogenous paste. For mechanical characterization of the mortar, compressive and flexural tests were performed at different ages, according to ASTM C109 and EN 1015-11. Five cubic ($50 \times 50 \times 50 \text{ mm}^3$) and five prismatic ($40 \times 40 \times 160 \text{ mm}^3$) specimens were used for each test and at each age. Specimens were cured for seven days in a damp environment and then stored in the laboratory (20°C , 67% RH) until the age of 90 days.

The reinforcing material is a woven biaxial fabric mesh made of an alkali-resistance fiberglass (Mapegrid G220). The mesh size and area per unit of width are equal to $25 \times 25 \text{ mm}^2$ and $35.27 \text{ mm}^2/\text{m}$, respectively. Direct tensile tests were performed on dry fibers (5 specimens) to obtain their tensile strength and elastic modulus. A universal testing machine with a maximum load capacity of 10 kN and a rate of 0.3 mm/min were used for these tests.

2.2 Bond characterization test

The single-sided pull-out test setup developed by the authors (Dalalbashi et al., 2018a) is used again in this study for investigating the fiber-to-mortar bond performance. The specimens consist of fibers embedded in disk shaped mortar with a thickness of 16 mm (see Figure 1). The free length of the fiber is embedded in an epoxy resin block with a rectangular cross-sectional area of $10 \times 16 \text{ mm}^2$, as shown in Figure 1, to facilitate gripping during the tests. For detailed information on the procedure followed for preparation of the specimens, the reader is referred to (Dalalbashi et al., 2018a). The specimens are demolded after 72 hours of preparation and are cured in a damp environment for seven days. After that, the specimens are stored in the lab environmental conditions (20°C , 67% RH) until the age of 90 days. The bonded length

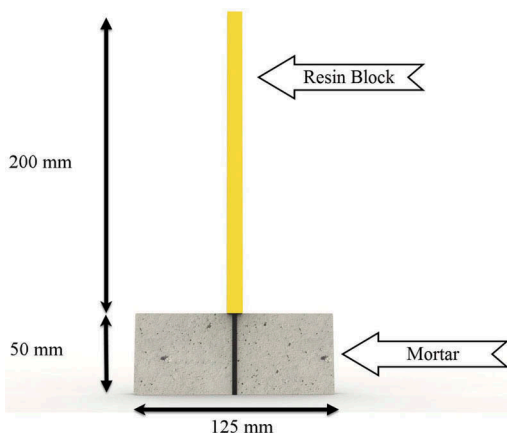


Figure 1. Pull-out specimen details.

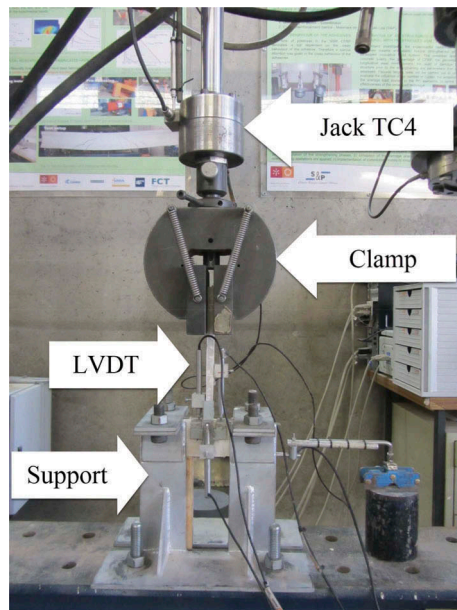


Figure 2. Pull-out test setup details.

of the glass fibers was 50 mm as it was previously reported to be around the effective bond length of this TRM system (Dalalbashi et al., 2018b).

For performing the tests, a u-shape steel support was used for fixing the specimens to a rigid frame. A mechanical clamp was used to grip the epoxy resin (and thus the fiber) from the top and performing the tests (Figure 2). Three LVDTs with 20 mm range and $2\text{-}\mu\text{m}$ sensibility were located at both sides of the epoxy block to record the slip. The average of these LVDT measurements is presented as the slip in the experimental results. All the tests were carried out using a servo-hydraulic system with a maximum capacity of 25 kN at a displacement rate of 1.0 mm/min.

2.3 Freeze-thaw exposure

After 90 days of curing, the specimens were stored in a climatic chamber and exposed to freeze-thaw cycles as shown in Figure 3. The cycles include thawing of the samples for 2 hours at 30°C and 90% RH and then freezing at -10°C for 2 hours. Between the thawing and freezing periods, the temperature was varied at the rate of $0.111^\circ\text{C}/\text{min}$. This cycle is repeated for 360 times. In the absence of proper standards, the temperature range of freeze-thaw cycles was selected from the literature (Ghiassi, Oliveira, & Lourenc, 2014; Uranjek & Bokanbosiljkov, 2015). This allows to compare the durability of two common strengthening systems (TRM vs. FRP).

At each 40 days (around 60 cycles) and when the chamber temperature was at 20°C , five specimens were taken from the climatic chamber to perform post-exposure tests. Generally, 45 specimens were tested in which 15 specimens were tested as control specimens and 30 were exposed to freeze-thaw

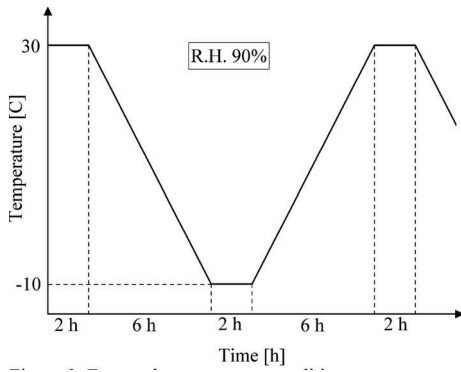


Figure 3. Freeze-thaw exposure condition.

cycles. The specimens were initially weighed and visually inspected. Then, the specimens were stored in environmental lab conditions for 7 days before testing (Maljaee et al., 2016). The post-exposure tests include pull-out tests and mechanical tests on the constituent materials (mortar and glass yarns).

3 RESULTS AND DISCUSSION

3.1 Material properties

The mean compressive and flexural strengths of the mortar as well as coefficient of variation in percentage (provided inside parentheses) after different exposure cycles were presented in Table 1. The average compressive strength of the control specimens (90-day mortar age) was found to be 16.76 MPa. It seemed that with exposure to freeze-thaw conditions, the compressive strength increased until 180 cycles, when it reaches its maximum value (19.48 MPa). At the same time, the compressive strength showed a less conspicuous (18.76 MPa). Comparison between the control and the exposure specimens showed that freeze-thaw cyclic caused the compressive strength to decrease slightly.

Table 1. Mortar mechanical properties under freeze-thaw cycles*.

Number of cycles	Compressive strength [MPa]	Flexural strength [MPa]
0 (control)	16.76 (12)	4.50 (2)
60	17.02 (11)	-
120	18.99 (25)	-
180	19.48 (6)	5.79 (6)
180 (control)	20.02 (14)	4.54 (14)
240	17.46 (4)	-
300	17.32 (2)	-
360	18.76 (3)	4.96 (5)
360 (control)	17.26 (11)	4.65 (7)

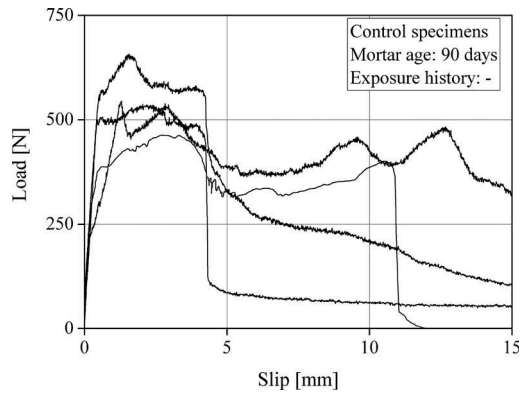


Figure 4. Pull-out response of the control specimens tested at zero cycle.

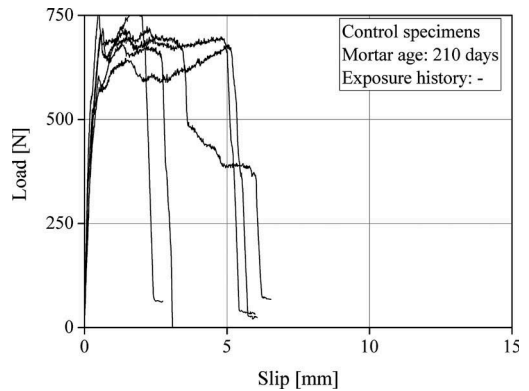


Figure 5. Pull-out response of the control specimens tested at 180 cycles (control).

Although the flexural strength was only measured at 180 and 240 cycles, the results show a similar trend as what was observed in the compressive tests. The flexural strength increased after 180 cycles (5.79 MPa) and it decreased afterwards. In addition, it was interesting to observe from Table 1 that freeze-thaw exposure led to increasing the flexural strength, especially at the 180-cycle point.

The average tensile strength, Young's modulus, and rupture strain of the control glass roving were 875 MPa (13 %), 65.94 GPa (5 %), and 1.77 % (10 %), respectively, with coefficients of variation provided inside parentheses. These values for the specimens exposed to 360 freeze-thaw cycles were 899 MPa (6 %), 70.72 GPa (3 %), and 1.86 % (8 %), respectively, showing no visible deterioration in the mechanical properties of the glass roving under considered exposure conditions and period.

3.2 Textile-to-mortar bond response

The experimental pull-out response of the control and freeze-thaw exposed samples were shown in Figure 7-6 and Figure 7-12, respectively. It can be observed that the bond strength of the control samples tested at

180 cycles (control) was larger than the samples tested at zero cycle (control). This could be due to the further curing of the mortar during this period. However, the bond strength decreased significantly after 360 cycles (control) of curing. The failure mode of

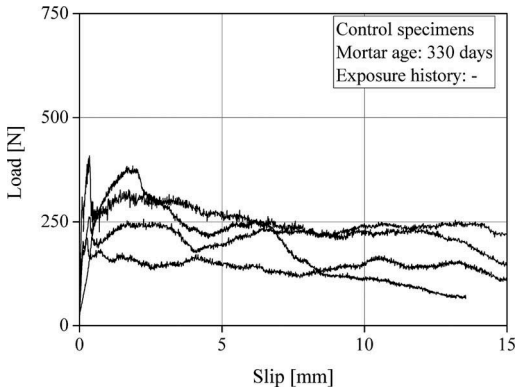


Figure 6. Pull-out response of the control specimens tested at 360 cycles (control).

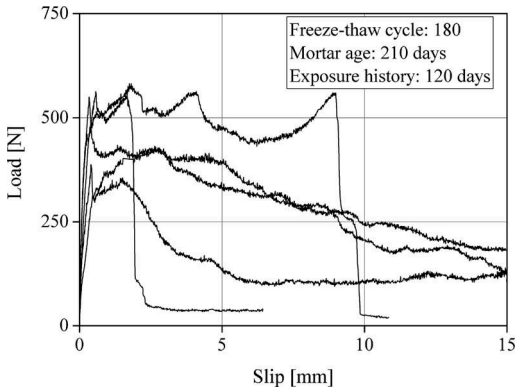


Figure 9. Pull-out response exposed to 180 cycles.

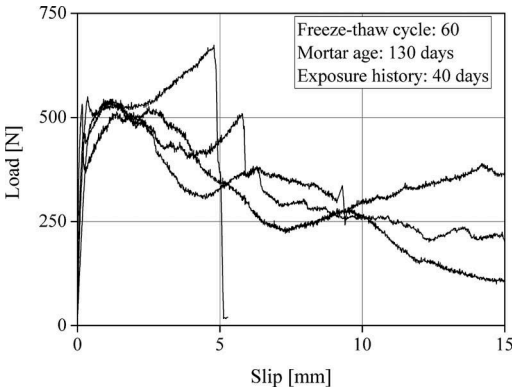


Figure 7. Pull-out response exposed to 60 cycles.

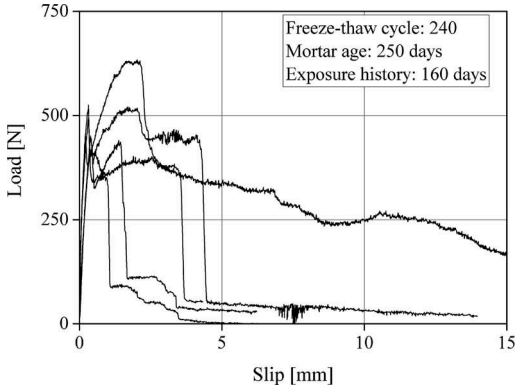


Figure 10. Pull-out response exposed to 240 cycles.

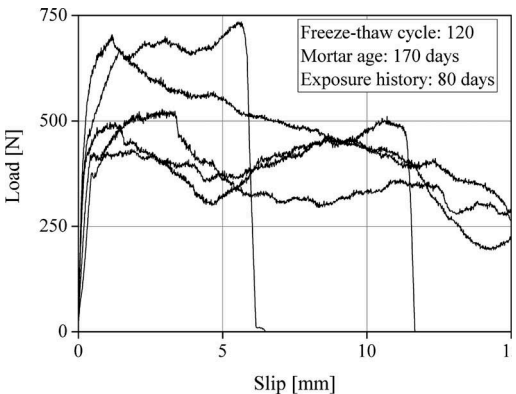


Figure 8. Pull-out response exposed to 120 cycles.

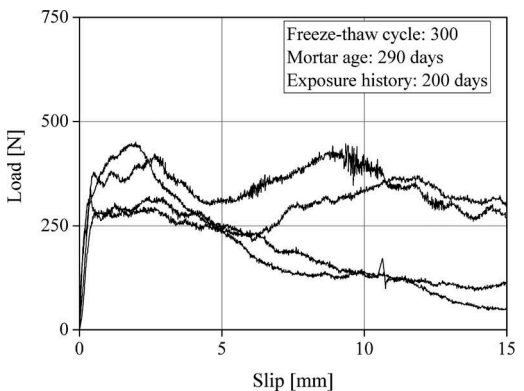


Figure 11. Pull-out response exposed to 300 cycles.

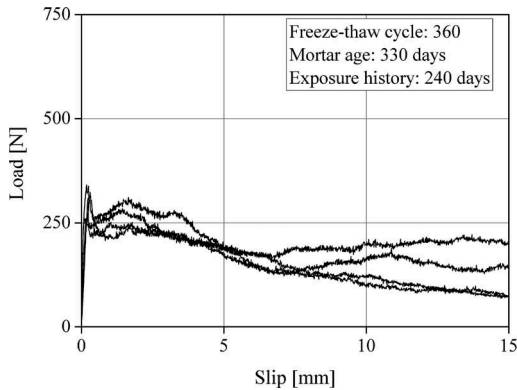


Figure 12. Pull-out response exposed to 360 cycles.

the samples also changed from the fiber slippage at the beginning (zero cycle) to rupture after 180 cycles (control) and again fiber slippage at 360 cycles (control).

As for the samples exposed to freeze-thaw conditions, a noticeable change of bond behavior could be observed by increasing the number of cycles. Until 240 cycles of exposure, the samples illustrated a negligible change in the bond strength. At this point (240 cycles), the bond strength between the fiber and the mortar showed a sudden decrease (that can be due to incremental damaged induced by previous freeze-thaw cycles) that causes the peak load to drop, in contrast to specimens exposed to fewer cycles. Afterwards, the bond strength decreased until the end of the exposure period. The failure mode of the samples changed from fiber slippage (until 180 cycles) to fiber slippage and rupture (at 240 cycles) then again to fiber slippage (at 300 and 360 cycles).

The main characteristics of the pull-out response of the samples (including peak load, slip corresponding to the peak load, the toughness and the initial stiffness) were summarized in Table 2. In addition, coefficients of variation in percentage were provided inside parentheses. The toughness or the absorbed energy defined as the area under the load-slip curve (Alwan, Naaman, & Hansen, 1991; Naik, Sharma, Chada, Kiran, & Sirotiak, 2019; Zhang, 1998).

It can be observed that the bond behavior was affected by both the freeze-thaw conditions and the mortar age. The bond properties of the exposure specimens showed a downward trend. For example, the peak load at the end of the freeze-thaw cycles reached to the minimum value. At the same time, the initial stiffness as well as the slip corresponding to the peak load was almost constant, while the pull-out energy decreased with time. In addition, the control specimens experience a similar behavior, so that the peak load decreased dramatically from 550.91 N to 308.41 N.

The pull-out behavior was similar to the observed changes in the mechanical properties of materials. For instance, the changes in the peak loads of both the control and the exposure specimens were in-line

Table 2. Effect of freeze-thaw conditions on the pull-out properties of glass-based TRM*.

FT cycle	S [mm]	P [N]	E [N.mm]	IS [N/mm]
0 (control)	2.10 (37)	551 (15)	4421 (35)	2049 (37)
60	0.73 (76)	540 (2)	4424 (28)	5297 (79)
120	1.69 (44)	567 (21)	5341 (24)	2815 (35)
180	0.5 (24)	468 (22)	3372 (47)	3639 (65)
180 (control)	0.64 (35)	692 (8)	2700 (36.8)	3006 (40)
240	0.34 (26.6)	470 (8)	1962 (77)	5476 (61)
300	1.86 (55)	384 (16)	3839 (30)	911 (19)
360	0.54 (112)	314 (8)	2605 (15)	2862 (46)
360 (control)	0.69 (114)	308 (28)	2950 (25)	1866 (69)

* FT: freeze-thaw; S: slip corresponding to peak load; P: peak load; E: energy; IS: initial stiffness.

with the observed changes of compressive strength of the mortar.

4 CONCLUSIONS

The effect of freeze-thaw conditions on the fabric-to-mortar bond behavior in a glass-based TRM composite system was experimentally investigated and discussed in this paper. The following conclusions can be drawn from the analysis of the obtained experimental results: (a) the environmental conditions generally reduced the bond properties of the glass-based TRM. For example, the peak load decreased by approximately 57 %. (b) The changes of the mortar strength seemed to be a good indication of the changes in the bond behaviour and were suggested to be considered in further investigations for estimating the long-term behavior of TRM systems.

More analysis should be performed to determine the contribution of the mortar age and the freeze-thaw environmental conditions to the degradation of the pull-out response as well as the mortar strength.

ACKNOWLEDGEMENTS

This work was partly financed by FEDER funds through the Competitvity Factors Operational Programme (COMPETE) and by national funds through

the Foundation for Science and Technology (FCT) within the scope of project POCI-01-0145-FEDER-007633. The support to the first author through grant SFRH/BD/131282/2017 is kindly acknowledged.

REFERENCES

- Al-jaberi, Z. K., & Myers, J. J. (2018). Effect of long-term environmental exposure on EB-FRP or FRCM-reinforced masonry system. In G. Milani, A. Taliercio, & S. Garrity (Eds.), *10th International Masonry Conference*. Milan.
- Alwan, J. M., Naaman, A., & Hansen, W. (1991). Pull-Out work of steel fibers from cementitious composites : analytical investigation. *Cement & Concrete Composites*, *13*, 247–255. [https://doi.org/10.1016/0958-9465\(91\)90030-L](https://doi.org/10.1016/0958-9465(91)90030-L).
- Carozzi, F. G., & Poggi, C. (2015). Mechanical properties and debonding strength of Fabric Reinforced Cementitious Matrix (FRCM) systems for masonry strengthening. *Composites Part B: Engineering*, *70*, 215–230. <https://doi.org/10.1016/j.compositesb.2014.10.056>.
- D'Antino, T., & Papanicolaou, C. (2017). Mechanical characterization of textile reinforced inorganic-matrix composites. *Composites Part B: Engineering*, *127*. <https://doi.org/10.1016/j.compositesb.2017.02.034>.
- Dalalbashi, A., Ghiassi, B., Oliveira, D. V., & Freitas, A. (2018a). Effect of test setup on the fiber-to-mortar pull-out response in TRM composites: experimental and analytical modeling. *Composites Part B: Engineering*, *143*, 250–268. <https://doi.org/10.1016/j.compositesb.2018.02.010>.
- Dalalbashi, A., Ghiassi, B., Oliveira, D. V., & Freitas, A. (2018b). Fiber-to-mortar bond behavior in TRM composites: effect of embedded length and fiber configuration. *Composites Part B: Engineering*, *152*, 43–57. <https://doi.org/10.1016/j.compositesb.2018.06.014>.
- Dalalbashi, A., Ghiassi, B., & Oliveira, D. V. (2019). Textile-to-mortar bond behaviour in lime-based textile reinforced mortars. *Construction and Building Materials*, *227*, 116682. <https://doi.org/10.1016/j.conbuildmat.2019.116682>.
- Donnini, J., Chiappini, G., Lancioni, G., & Corinaldesi, V. (2019). Tensile behaviour of glass FRCM systems with fabrics' overlap: Experimental results and numerical modeling. *Composite Structures*, *212* (October2018), 398–411. <https://doi.org/10.1016/j.compstruct.2019.01.053>.
- Ghiassi, B., Oliveira, D. V., & Lourenc, P. B. (2014). *Hygrothermal durability of bond in FRP-strengthened masonry*. 2039–2050. <https://doi.org/10.1617/s11527-014-0375-7>.
- Ghiassi, B., Oliveira, D. V., Marques, V., Soares, E., & Maljaee, H. (2016). Multi-level characterization of steel reinforced mortars for strengthening of masonry structures. *Materials and Design*, *110*, 903–913. <https://doi.org/10.1016/j.matdes.2016.08.034>.
- Ghiassi, B., Xavier, J., Oliveira, D. V., Kwiciecien, A., Lourenço, P. B., & Zajac, B. (2015). Evaluation of the bond performance in FRP-brick components re-bonded after initial delamination. *Composite Structures*, *123*, 271–281. <https://doi.org/10.1016/j.compstruct.2014.12.047>.
- Heshmati, M., Haghani, R., & Al-Emrani, M. (2017). Durability of CFRP/steel joints under cyclic wet-dry and freeze-thaw conditions. *Composites Part B: Engineering*, *126*, 211–226. <https://doi.org/10.1016/j.compositesb.2017.06.011>.
- Maljaee, H., Ghiassi, B., Lourenço, P. B., & Oliveira, D. V. (2016). FRP– brick masonry bond degradation under hygrothermal conditions. *Composite Structures*, *147*, 143–154. <https://doi.org/10.1016/j.compstruct.2016.03.037>.
- Mazzuca, S., Hadad, H. A., Ombres, L., & Nanni, A. (2019). Mechanical Characterization of Steel-Reinforced Grout for Strengthening Existing Masonry and Concrete Structures. *Journal of Materials in Civil Engineering*, *31*(5), 04019037. [https://doi.org/10.1061/\(ASCE\)MT.1943-5533.0002669](https://doi.org/10.1061/(ASCE)MT.1943-5533.0002669).
- Naik, D. L., Sharma, A., Chada, R. R., Kiran, R., & Sirotiak, T. (2019). Modified pullout test for indirect characterization of natural fiber and cementitious matrix interface properties. *Construction and Building Materials*, *208*, 381–393. <https://doi.org/10.1016/j.conbuildmat.2019.03.021>.
- Papanicolaou, C. G., Triantafillou, T. C., Papathanasiou, M., & Karlos, K. (2007). Textile reinforced mortar (TRM) versus FRP as strengthening material of URM walls: out-of-plane cyclic loading. *Materials and Structures*, *41*(1), 143–157. <https://doi.org/10.1617/s11527-007-9226-0>.
- Razavizadeh, A., Ghiassi, B., & Oliveira, D. V. (2014). Bond behavior of SRG-strengthened masonry units: Testing and numerical modeling. *Construction and Building Materials*, *64*, 387–397. <https://doi.org/10.1016/j.conbuildmat.2014.04.070>.
- Uranjek, M., & Bokan-bosiljkov, V. (2015). Influence of freeze – thaw cycles on mechanical properties of historical brick masonry. *Construction and Building Materials*, *84*, 416–428. <https://doi.org/10.1016/j.conbuildmat.2015.03.077>.
- Younis, A., & Ebead, U. (2018). Bond characteristics of different FRCM systems. *Construction and Building Materials*. <https://doi.org/10.1016/j.conbuildmat.2018.04.216>.
- Zhang, S. Y. (1998). Debonding and cracking energy release rate of the fiber/matrix interface. *Composites Science and Technology*, *58*(3–4), 331–335. [https://doi.org/10.1016/S0266-3538\(97\)00073-0](https://doi.org/10.1016/S0266-3538(97)00073-0).